# EXPERIMENTAL STUDY OF THE DETERMINATION OF DRY COMPACTION OF WARE SHAPED BY UNIDIRECTIONAL PRESSING, IN CONTINUOUS OPERATION AND IN TRUE TIME.

**by Blasco, A.; Llorens, D.; Mallol, G.; Jarque, J.C.**

Instituto de Tecnología Cerámica. Universitat Jaume I de Castellò.
Asociación de Investigación de las Industrias Cerámicas (AICE). Castellón (España)

## 1.- INTRODUCTION.

Shaping ceramic wall and floor tile is carried out by unidirectional dry pressing (H < 8%), given their regular geometry and high specific surface area/thickness ratio. Hydraulic presses are used for this purpose which confer enough mechanical strength on the ware for subsequent manipulation.

Modifications in the spray-dried powder characteristics (grain size, moisture content, etc.) and the die-filling method itself, can give rise to differences in its load, which on pressing lead to differences in bulk density.

Bulk density of the ware will condition its behaviour in subsequent process stages (drying, glazing, firing, etc.), decisively affecting its quality.

## 2.- IMPORTANCE OF BULK DENSITY OF THE WARE AS CONTROL VARIABLE IN THE PRESSING STAGE.

The increasing finished product quality requirements of the last few years, have led to greater interest in determining the fundamental variables of the ceramic process and their effect on the end product. Studies conducted on these variables have made it possible to show that dry bulk density of the ware affects its behaviour in the different process stages (1) (2) (3) (4) (5) (Figure 1):

- Drying and glazing operations are highly influenced by dry bulk density of the pressed ware. In fact, both the drying rate (6) and suction capability (7) of the pressed ware have been shown to decrease as dry bulk density increased.

- Moreover, on raising compaction of the ware, its mechanical strength increases (5), raising performance of the silk screening operation and in general, of all those stages involving manipulation of the piece, or where it is subjected to mechanical stresses.

- The fact that the coefficient of effective diffusivity of the gases through the ware depends on its porosity (8), makes this value condition its behaviour during preheating, directly affecting oxidation of the organic matter to be found there.

- The maximum degree of sintering reached in the firing stage, considerably depends upon dry bulk density of the ware. In fact, on increasing compaction of the ware, for the same peak firing temperature, its water absorption capability and linear shrinkage (5) drops.

- During cooling, the body-glaze fit takes place, and planarity of the ware is determined. Greater or lesser adaptation in this firing stage depends, among other variables, on the similarity of Young's moduli for both layers and these are in function of their porosity (9).

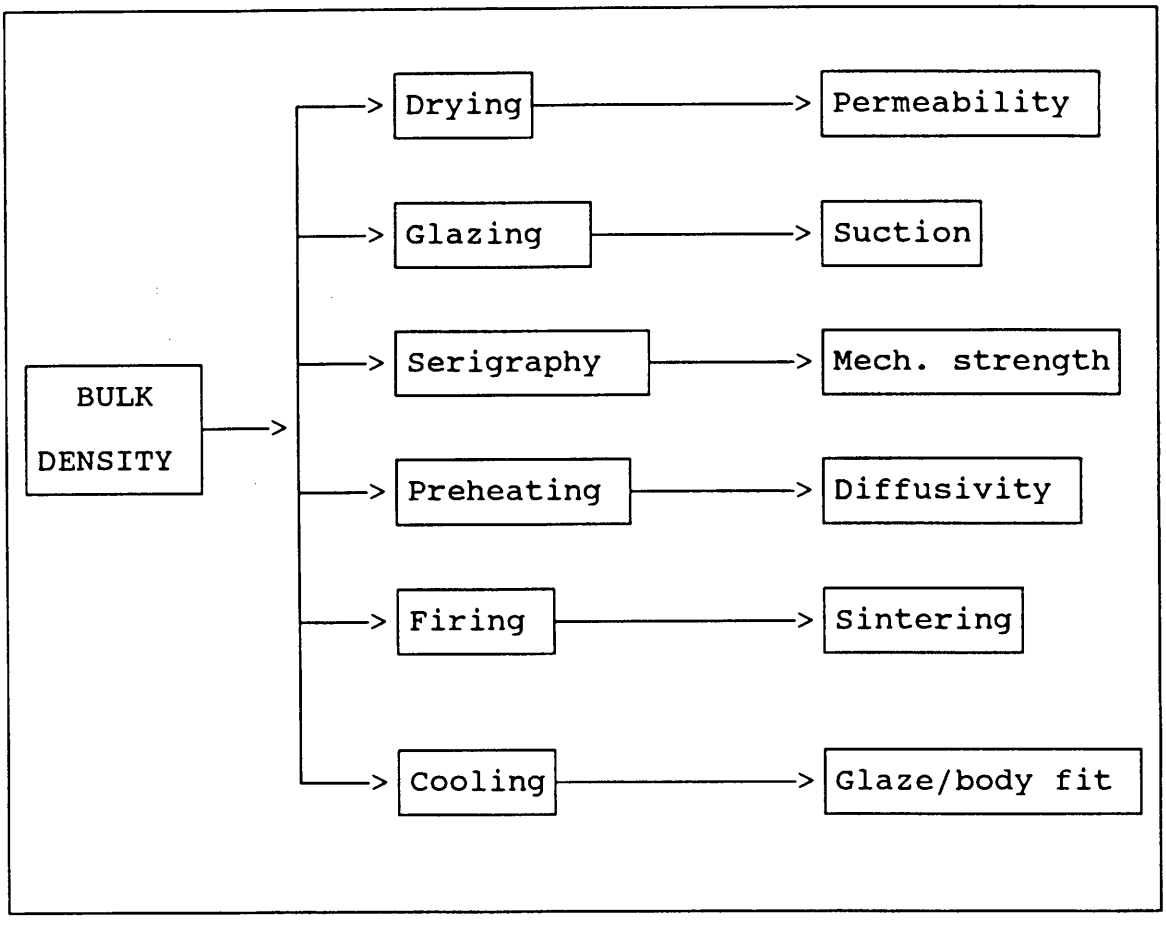


Figure 1.- Effect of bulk density on the different stages of the manufacturing process.

| CHARACTERISTICS OF THE FINAL PRODUCT | POSSIBLE DEFECTS |
|---|---|
| - Dimensional stability | - Wedging and deviating sizes and thickness |
| - Suitable porosity | - Lack of frost resistance |
| - Planarity | - Curvatures |
| - Aesthetic properties | - Crazing |

Figure 2.- Characteristics required in ceramic wall and floor tile.

From the foregoing, the conclusion may be drawn that thoroughgoing compaction control will lead to an increase in quality of the final product (Figure 2).

One of the main characteristics required in the finished product, is its dimensional stability. Analysis was conducted in the range of maximal variation in bulk density which still enables dimensions of the ware to be kept within required quality limits.

Lowering porosity during firing leads to shrinkage of the pieces which, for a certain composition and lacking temperature gradients in the kiln, is a function of bulk density of the unfired ware, as may be observed from Figure 3.

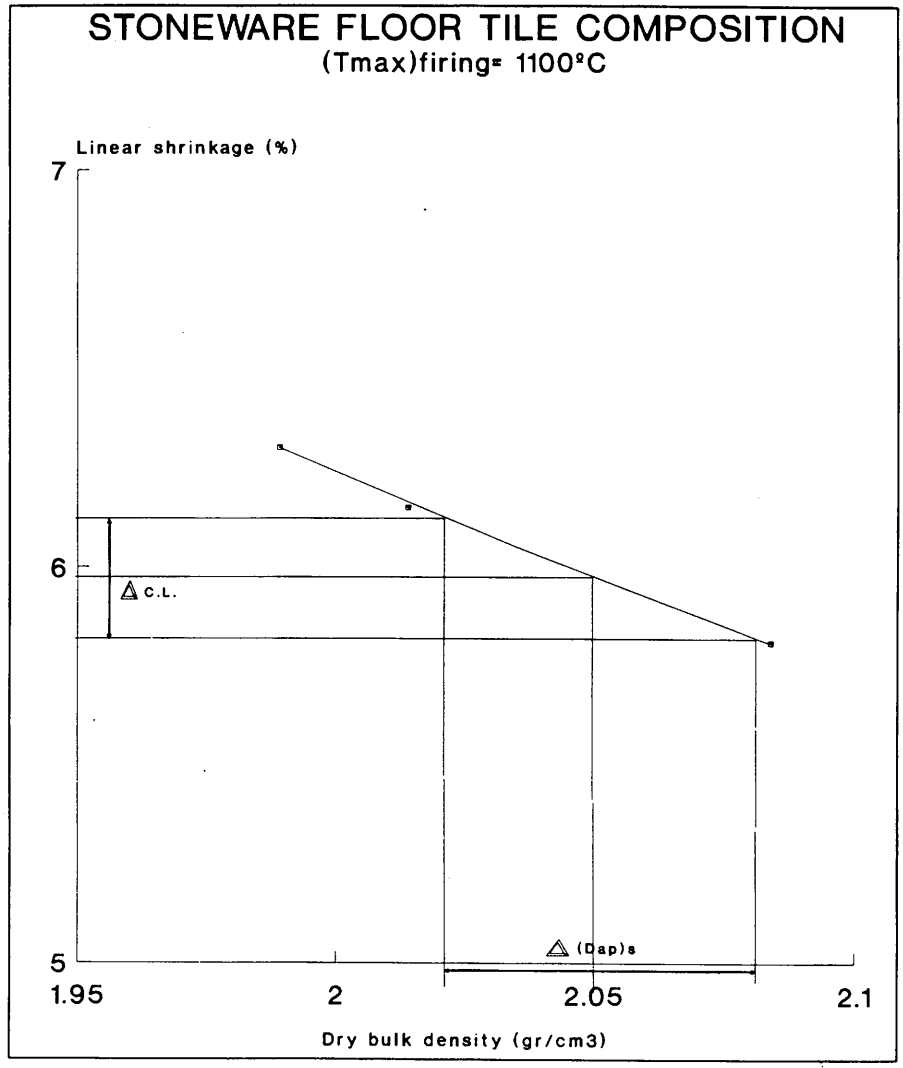


Figure 3.- Computation of the maximum bulk density variation interval

Therefore, lack of intrinsic dimensional homogeneity (wedging) of a piece will depend on irregular compaction distribution inside it and the appearance of different facial dimensions (deviating sizes of the ware), will depend on unequal overall compaction among the pieces.

If mean work bulk density of 2.05 g/cm$^3$ is assumed, and absolute error in the dimensions of the final product is required to be less than ±0.5 mm, a maximum tolerated dry bulk density variation of 0.03 g/cm$^3$ (Figure 3) is found, for a stoneware floor tile composition measuring 330x330 mm, and fired at a maximum temperature of 1100°C.

This value gives some inkling of the high sensitivity of the variable, and the need to use an accurate method in determining it.

## 3.- AIM OF THIS RESEARCH.

The aim of the present study is to evaluate the different methods used at present in determining bulk density and to apply the one considered best, according to the selection criteria detailed in Section 5, to the shaping of ceramic ware by the pressing process.

## 4.- EXPERIMENTAL TECHNIQUES FOR MEASURING COMPACTION.

The methods for determining bulk density which were analyzed are described below:

### 4.1.- Gamma ray absorption.

This involves determining the attenuation of $N_o$ intensity gamma ray radiation, across a ceramic piece (10). Computation of bulk density of the ware is conducted from the equation:

$$\rho = \frac{1}{\mu * x} \ln \left(\frac{N_o}{N}\right) \qquad (1)$$

where:

$\mu$ : absorption coefficient (cm /g)
x : thickness of the piece (cm)
$N_o$ : initial intensity of gamma radiation
N : intensity of gamma radiation after crossing the piece
$\rho$ : bulk density of the piece (g/cm$^3$)

As the absorption coefficient is independent of porosity, and is solely a function of the composition of the material and radiation intensity, it can be computed by determining bulk density of a piece indirectly and subsequently subjecting it to a radiological test.

The equipment needed is a gamma ray source with a radiation detector, while the sample to be tested, whose thickness (x) will have been determined beforehand, is located between them (Figure 5).

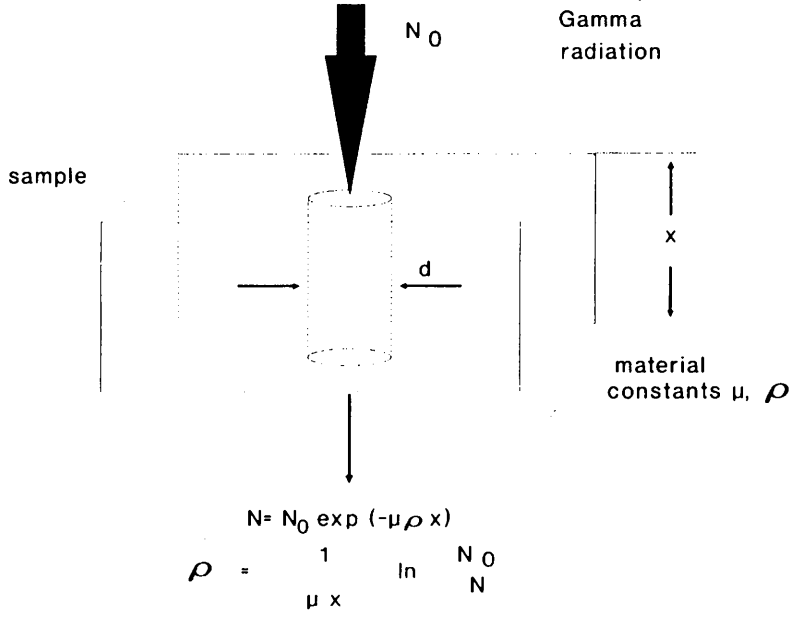


Figure 4.- Basis for the bulk density determination method by gamma ray absorption.

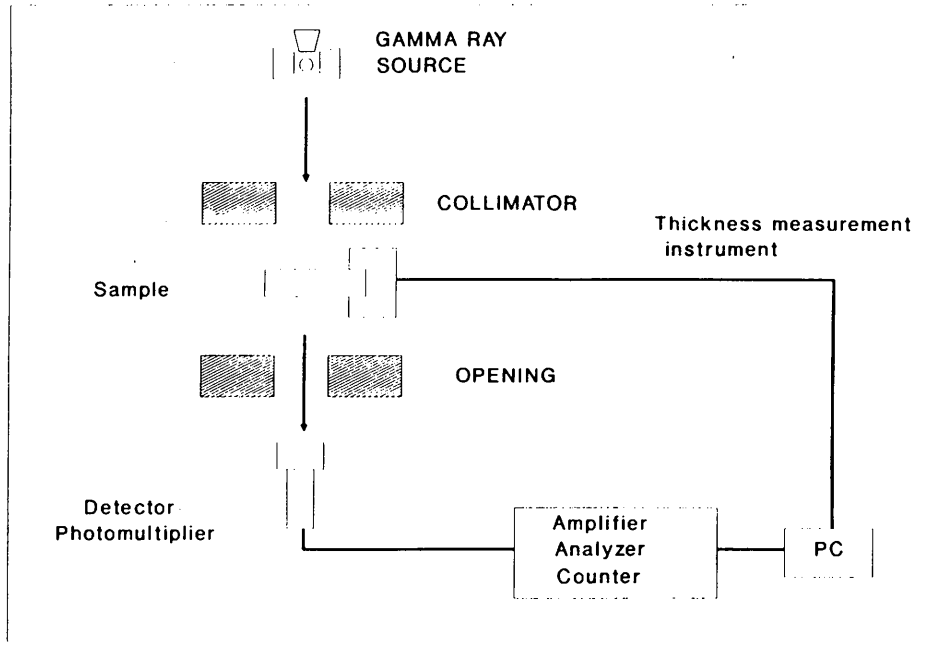


Figure 5.- Scheme of the setup used in determining bulk density by gamma rays.

### 4.2.- Ultrasounds.

The method involves measuring the propagation rate of an ultrasonic wave across a ceramic piece. Its bulk density is computed from the following equation:

$$\rho = \frac{E}{v^2} * \frac{(1-\mu)}{(1+\mu)\ (1-2-*\mu)} \qquad (2)$$

where:

- $\rho$ : bulk density of the piece (g/cm$^3$)
- E : Young's modulus (N/m )
- v : velocity of the wave in the solid (m/s)
- $\mu$ : Poisson's modulus

Variation of Poisson's modulus with porosity is small (15), however it markedly affects the value of Young's modulus (20). In the case being studied, it can be computed from the following equation:

$$E = E_o * \exp(- b * \varepsilon) \qquad (3)$$

where:

- $E_o$ : Young's modulus of the non-porous solid (N/m )
- $\varepsilon$ : porosity
- b : empirical constant

Porosity is related to bulk density by means of the equation:

$$\varepsilon = 1 - \frac{\rho}{\rho_r} \qquad (4)$$

where:

- $\rho_r$ = solid density (g/cm$^3$)

Laboratory tests allow the curves E = f (ε) from which b and $E_o$ are computed to be obtained, for a certain composition. By substituting these values in Equation (3) and combining this with Equation (2), an equation is obtained with which bulk density of the piece is computed.

The measuring apparatus basically consists of an electric pulse source, and a generator and receiver of ultrasounds (Figure 6). In order to achieve good wave propagation/piece, some substance facilitating it must be inserted between both surfaces, such as water, gel, grease, etc (14).

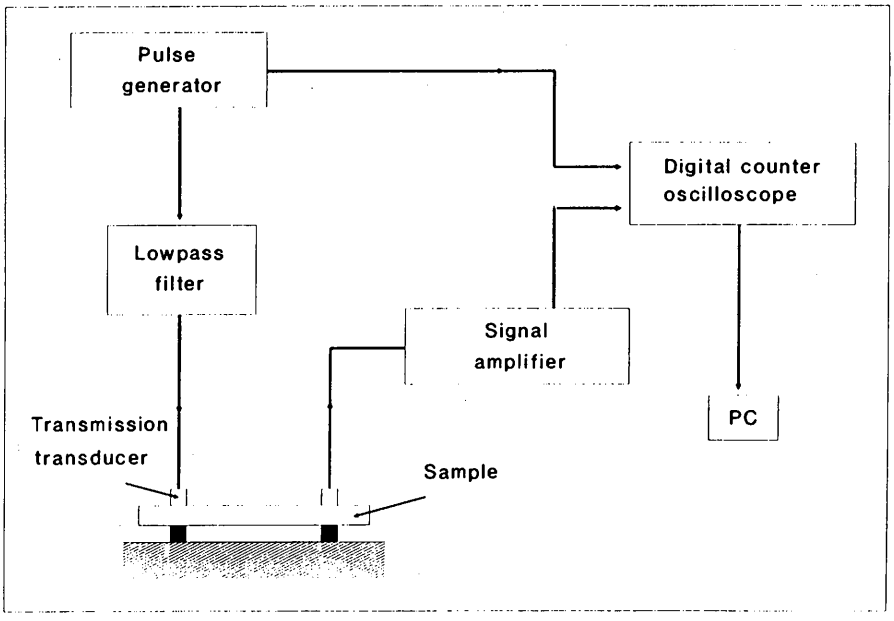


Figure 6.- Scheme of the assembly used in determining bulk density by ultrasounds.

### 4.3.- X-ray inspection.

This involves determining the attenuation produced in the beam of photons Io on crossing a solid body (11) (12). Solid density may be computed by means of the equation:

$$\rho = \frac{1}{ß * x} \ln \left(\frac{Io}{I}\right) \qquad (5)$$

where:

- ρ : solid density (g/cm³)
- x : thickness of the sample (cm)
- $I_o$ : intensity of the incident photon beam (1/sec)
- I : intensity of the photon beam after crossing the piece (1/sec)
- ß : coefficient of mass absorption (cm /g)

The coefficient of mass absorption depends on the radiation energy and the chemical composition of the sample (12), whilst being independent of density.

### 4.4.- Extensometry.

This involves determining the pressing force in the pressing die and its correlation with bulk density from the equation:

$$\rho = a * \log (F/A) + b \qquad (6)$$

where:

ρ : density of the piece at the measuring point (g/cm³)
F : force measured by the transducer (Nw)
A : area over which compaction is determined (cm )
a + b : coefficients depending on moisture content and nature of the spray-dried powder.

The experimental setup involves force sensors located in the ram. Its impact on the powder bed leads to deformation of the sensor wafer, measurable and proportional to the force applied (16).

The coefficients "a" and "b" of Equation (6) depend on the nature of the spray-dried powder and its moisture content. Therefore, their determination entails the prior construction of the spray-dried powder compaction diagram. This consists of the plot of the variation in bulk density, determined by another method, with the applied force, measured by load sensors for different powder moisture contents (5).

### 4.5.- Immersion in mercury.

This method involves measuring the upthrust a solid undergoes on submerging it in liquid, in this case in mercury (17).

The equation used is:

$$\rho = \rho_{Hg} * \frac{m_p}{e} \qquad (7)$$

where:

ρ : density of the sample tested (g/cm³)
$\rho_{Hg}$ : density of mercury (g/cm³.)
$m_p$ : dry mass of the sample (g)
e : upthrust of the sample submerged in mercury (g)

The experimental setup used (patented by A.I.C.E.) allows immersion of the sample in mercury and the computation of the upthrust it undergoes (Figure 7).

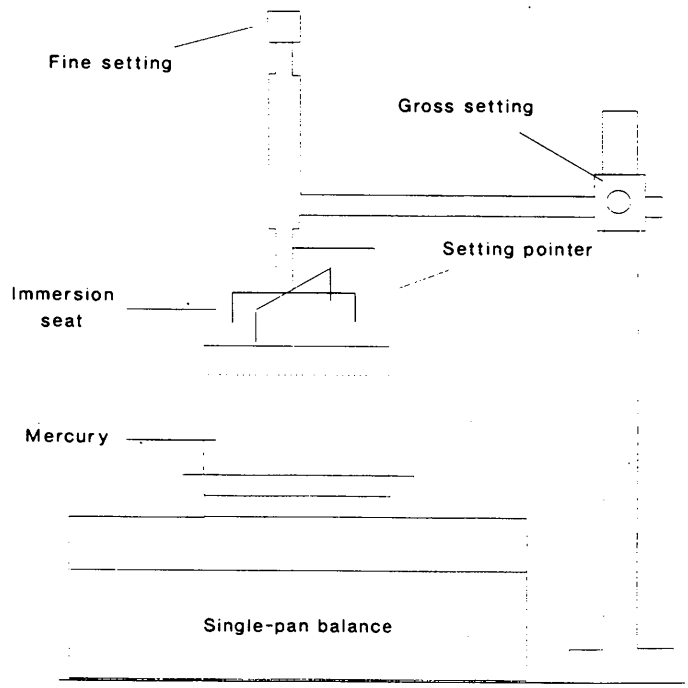


Figure 7.- Scheme of the setup for determining bulk density by immersion in mercury.

### 4.6.- Penetrometry.

This involves determining the force required to introduce the constant length of a pointer attached to a metal rod, in the region whose bulk density is to be determined. The maximum force used in this operation is proportional, at a first aproximation, to the compaction of the region explored.

## 5.- SELECTION OF THE MEASURING METHOD. SELECTION CRITERIA.

The criteria taken into account on choosing the most suitable measuring method to carry out the determinations on an industrial scale were:

- Rapidity. Thus making it possible to obtain data in true time.
- Integral. Allowing analysis of sufficiently representative areas of the piece.
- Non-destructive. Enabling bulk density analysis of all the pieces to be carried out.
- Low costs. Not involving excessive increase in pressing operation costs.
- Safety of the operation.
- Constructive simplicity of the facility, its installation and its use.
- Independence with regard to the remaining process variables.

Table I details the valuation of each parameter for the different analytical methods appraised.

| Method | Rapidity | Integral | Complexity | | | Ind.other var. | | Destr. | Costs | Harmful | Mean Value |
|---|---|---|---|---|---|---|---|---|---|---|---|
| | | | Cons | Ins | Use | T | Moist. | | | | |
| Immersion in mercury | 0 | 2 | 2 | 2 | 2 | 1 | 0 | 0 | 2 | 1 | 7.5 |
| Radiology | 2 | 2 | 0 | 2 | 2 | 2 | 0 | 2 | 0 | 0 | 8.3 |
| Penetrometry | 1 | 0 | 2 | 2 | 2 | 2 | 0 | 1 | 2 | 2 | 9.0 |
| Extensometry | 2 | 1 | 0 | 0 | 2 | 1 | 2 | 2 | 0 | 2 | 9.2 |
| Gamma ray absorption | 2 | 0 | 0 | 2 | 2 | 2 | 0 | 2 | 0 | 0 | 6.3 |
| Ultrasounds | 1 | 1 | 0 | 2 | 0 | 1 | 0 | 0 | 0 | 1 | 4.2 |

(*) the grading scheme was:
0 : Unsuitable 1 : Suitable 2 : Excellent

Table I.- Valuation of the methods described.

As a result of this first assessment, the ultrasonic, gamma ray absorption and mercury immersion methods were eliminated. Of the three methods left, penetrometry was considered the least advisable as too localized a method was involved which was not very accurate (18).

Finally, the study focused on the extensometric method, because unlike the radiological method, besides assessment of the compaction of the piece it also allowed analysis of pressing process dynamics, as data is provided on the pressing application mode with time.

## 6.- DESCRIPTION OF THE MEASURING SYSTEM.

The physical principle used in determining force, is the change which takes place in the nominal resistance of certain conductors when they are deformed by means of force. This is determined by using force sensors based on strain gauges.

This change in resistance, proportional to the deformation, can be determined by using the electrical resource of a Wheatstone bridge, and the applied force can therefore be accurately established.

In order to determine pressure on the analyzed regions of the spray-dried powder bed at each moment, a commercial force sensor was placed inside one of the upper rams of a hydraulic press.

A cylindrical seat and openings into which ducts lead for the connecting wires to pass through, were mechanized in the block. An opening was made in the ram through which the sensor rod reached the bottom plane of the vulcanized rubber lining (Figure 8).

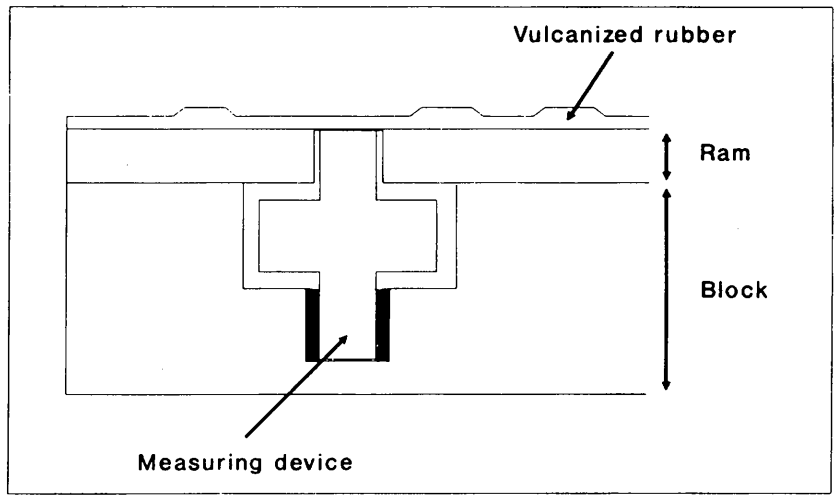


Figure 8.- Location of the sensor inside the ram.

In view of the great number of kinds of sensors available on the market, choosing a suitable sensor required taking into account the peculiar characteristics of the measuring chamber:

- Reduced space.
- High mechanical fatigue (100 cycles/hr at a peak pressure of 250-400 kg/cm ).
- Work temperature (maximum of 70°C).
- Electromagnetic environment.

The sensor was conveniently wired for transmitting electric signals to the data processing system amplifier. This was then digitalized by means of an analog-to-digital converter, displayed on a PC screen and/or stored in a disc unit for later detailed study (Figure 9).

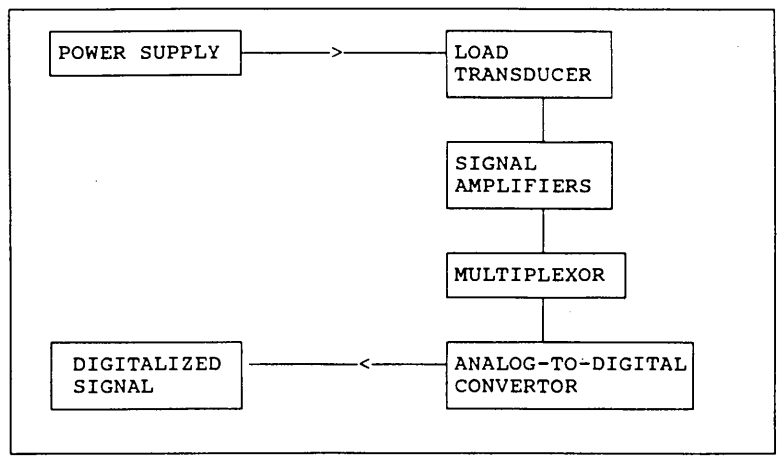


Figure 9.-Scheme of the system used in determining the force exerted on localized areas of the ceramic ware.

## 7.- MEASURING EQUIPMENT RESPONSE.

A series of laboratory experiments was run to verify the appropriate functioning of the setup.

To begin with, increasing known forces were applied on the sensor-monitored area, by means of a universal testing machine. By plotting the value of the maximum applied force (F(KNw) in function of the signal received (S(digits), the following plot was obtained:

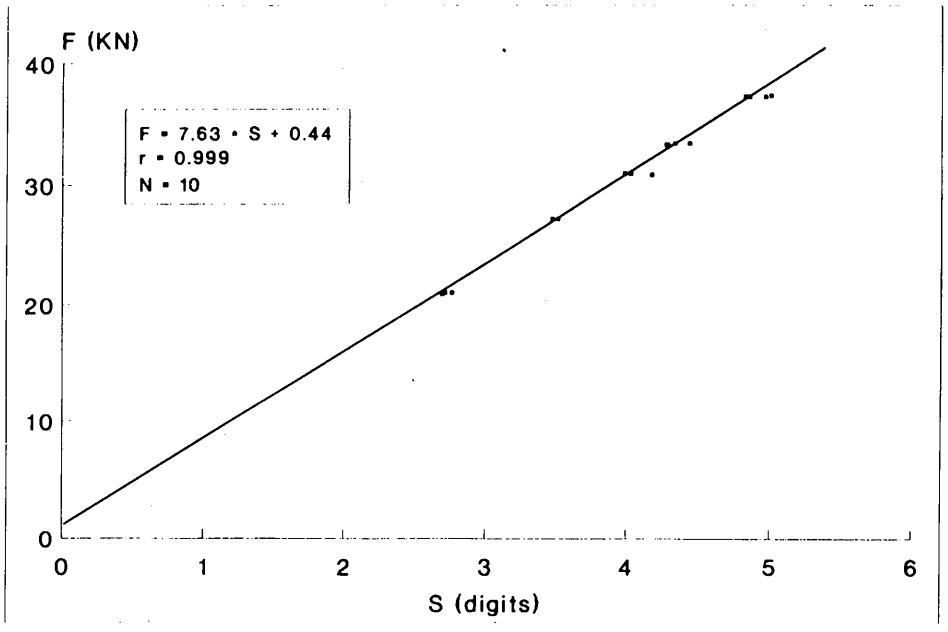


Figure 10.- Correlation between the force applied and the signal received by the data processing system.

The high correlation corroborated the suitability of the sensor for measuring the applied force.

The fact that an ordinate is found at the origin for this relation, implies there being a threshold force (0.44 KNw) below which the sensor does not perceive any signal. This is due to the force attenuating effect the vulcanized rubber has at low pressures.

Another experiment carried out in the laboratory was spray-dried powder compaction over the sensor-monitored area, at different pressures. The assembly used was a cylindrical die which, suitably arranged over the sensor-monitored area, was filled with spray-dried powder with a moisture content similar to that of industrial powders. A piston, to which a variable force was applied, transmitted this to the powder, increasing compaction (Figure 11).

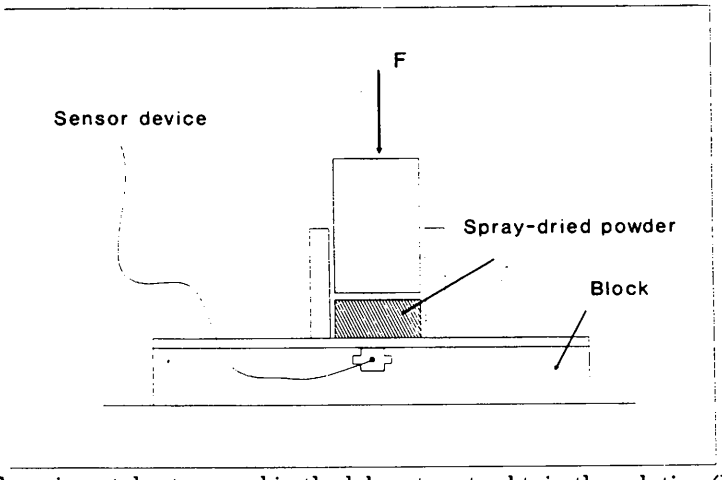


Figure 11.- Experimental setup used in the laboratory to obtain the relation (Dap)s = f(log(F))

Subsequently bulk density of the shaped test pieces was determined by the mercury immersion method and was correlated with the logarithm of the force, yielding the following plot:

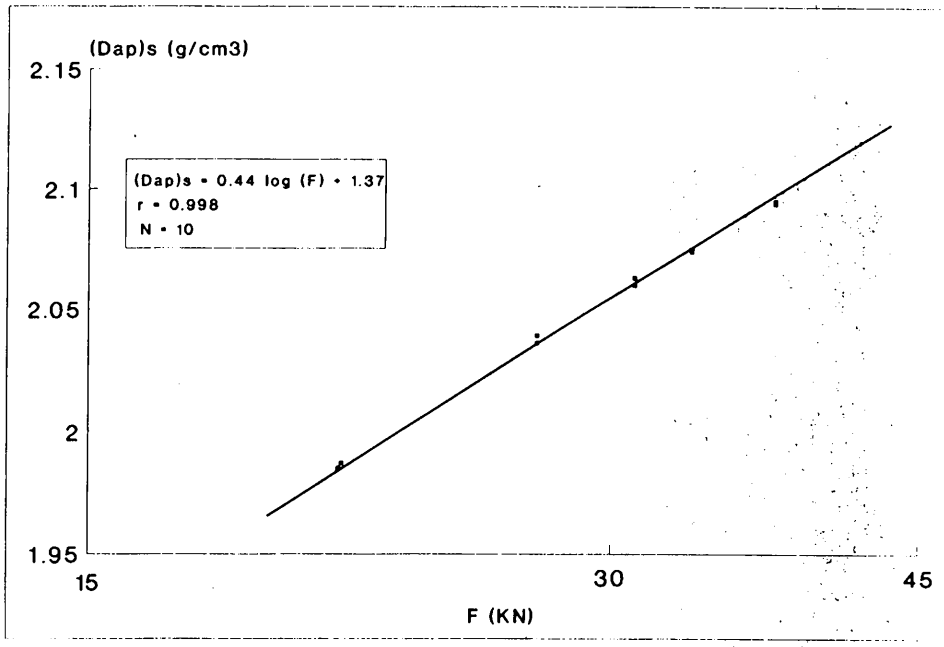


Figure 12.- Correlation between force and bulk density in the sensor-monitored area.

On corroborating the validity of the method in the laboratory, it was then tested on an industrial scale.

## 8.- THE UNIDIRECTIONAL PRESSING OPERATION: PROCESS MONITORING

The pressing cycle involves the set of operations conducted by the press during compression.

This cycle was monitored and the information was obtained graphically, plotting the position of the feeding system and the frame at each moment, as well as pressure evolution in the main cylinder and force inside the die, in function of time.

The compression cycle started with die-filling by the loading system (Figure 13) and withdrawal of the shaped ware from the previous cycle.

When withdrawal of the feeding system had freed the way for the frame, this descended, braking a moment before colliding with the powder to attenuate impact sharpness, followed by the first pressing, increasing pressure in the hydraulic circuit. The force was registered by the sensor device located inside the die.

After the first pressing period had ended, the frame was lifted, releasing the air trapped in the pressing chamber for a period of time ($t_D$), thus avoiding the problems inherent to the presence of trapped air in the compact.

After de-airing, the frame dropped once more, progressively increasing pressure in the main cylinder and force in the die until the assigned pressure was reached. After holding this for the preset time, the second pressing ended.

Commutation of the oil in the hydraulic system leads to raising of the frame, starting the extraction stage, with the rise of the lower rams.

When the frame had risen sufficiently and the lower rams were completely lifted, a new pressing cycle started with loading of the dies.

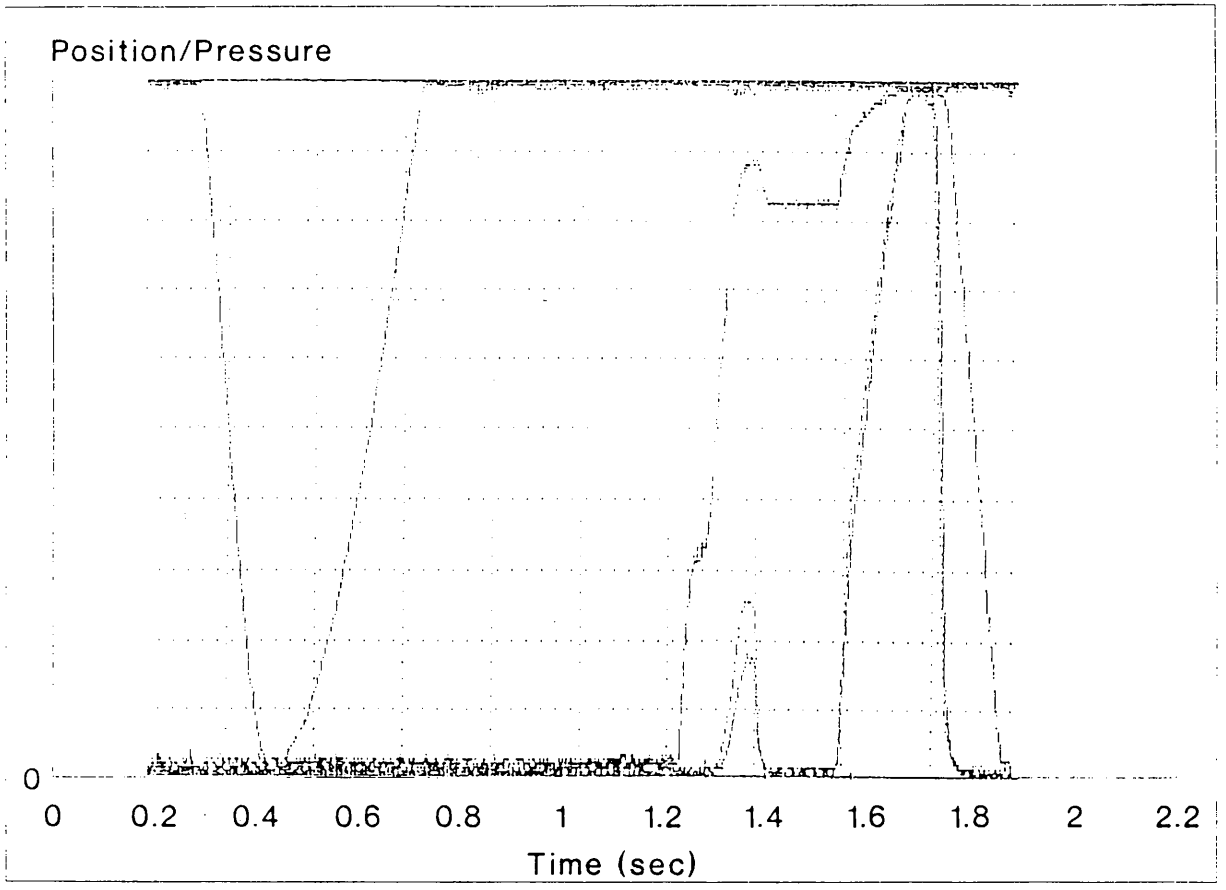


Figure 13.- Monitoring of the pressing cycle.

## 9.- RESULTS.

The experiments on an industrial scale were carried out over a total of 17 days (103,000 strokes at peak assigned pressure of 290 kg/cm ), without any physical deterioration in the sensor being observed.

Wares were pressed at different pressures, and the signal received from the sensor in different samplings was processed. Subsequently, moisture content of the pieces was computed, as was their bulk density in the sensor-monitored area, by the mercury immersion method.

A plot was then made of dry bulk density versus the logarithm of maximum force (computed from the signal recorded for maximum pressure in the second pressing), from the experimental data. The plots obtained are reported in Figures 14 and 15, and the values obtained after fitting by linear regression are listed in Table II.

The slope (M) and the ordinate at the origin (b) of these equations are a function of the moisture content (5), for a spray-dried powder with the same grain-size distribution and nature. In Figures 16 and 17, the variation of the slope and the ordinate at the origin are plotted in function of moisture content, determined for each day of experiments, on a double-logarithmic scale.

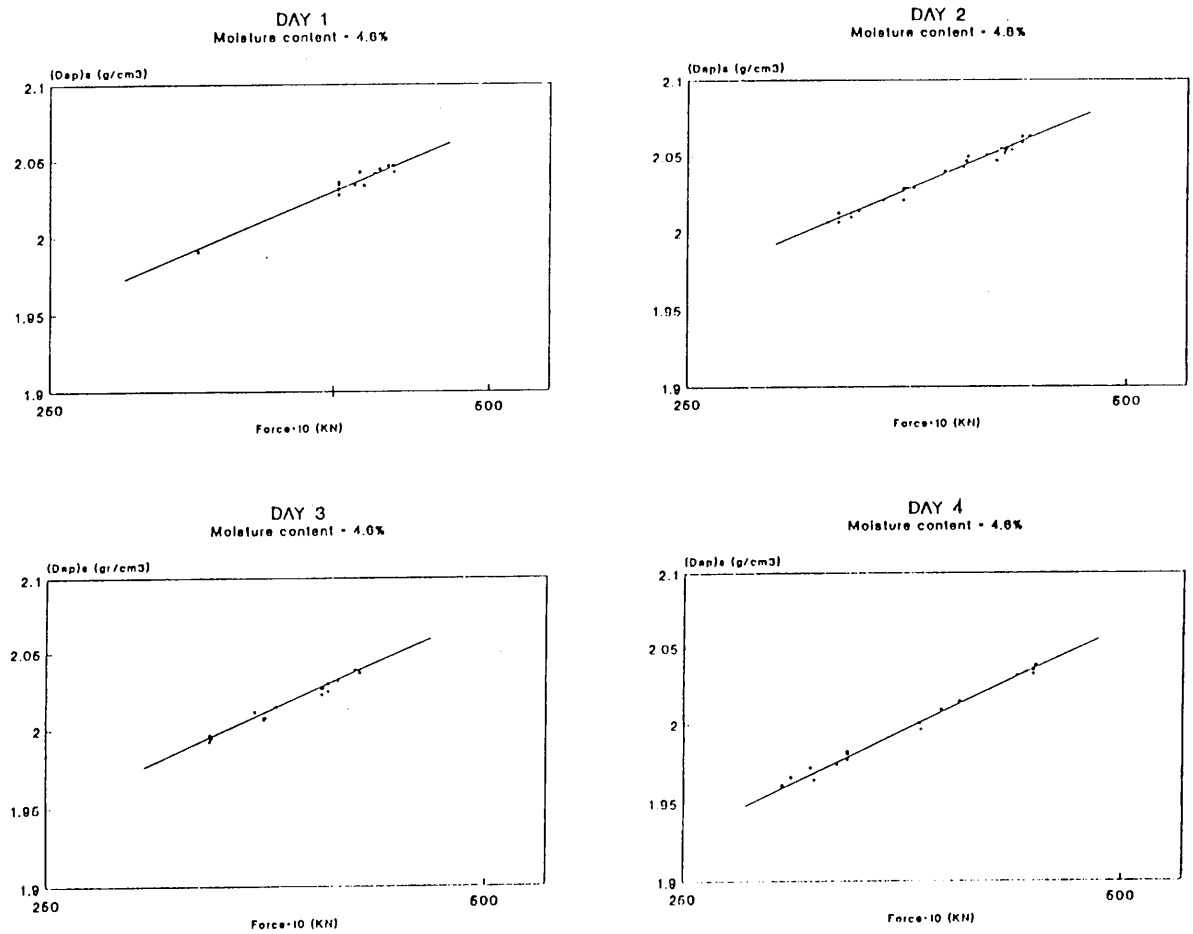


Figure 14.-Correlations between force, measured by the sensor, and dry bulk density determined by immersion in mercury.

| DAY | H (%) | M | b | r | N |
|---|---|---|---|---|---|
| 1 | 4.6 | 0.41 | 1.38 | 0.975 | 13 |
| 2 | 4.8 | 0.40 | 1.41 | 0.989 | 26 |
| 3 | 4.6 | 0.41 | 1.37 | 0.987 | 17 |
| 4 | 4.6 | 0.43 | 1.33 | 0.995 | 17 |
| 5 | 4.5 | 0.42 | 1.34 | 0.991 | 19 |
| 6 | 4.5 | 0.45 | 1.30 | 0.998 | 7 |
| 7 | 4.7 | 0.39 | 1.40 | 0.996 | 9 |
| 8 | 4.4 | 0.44 | 1.32 | 0.990 | 15 |

Table II.- $(Dap)_s = f(\log(F))$ correlations for different days of experiments.

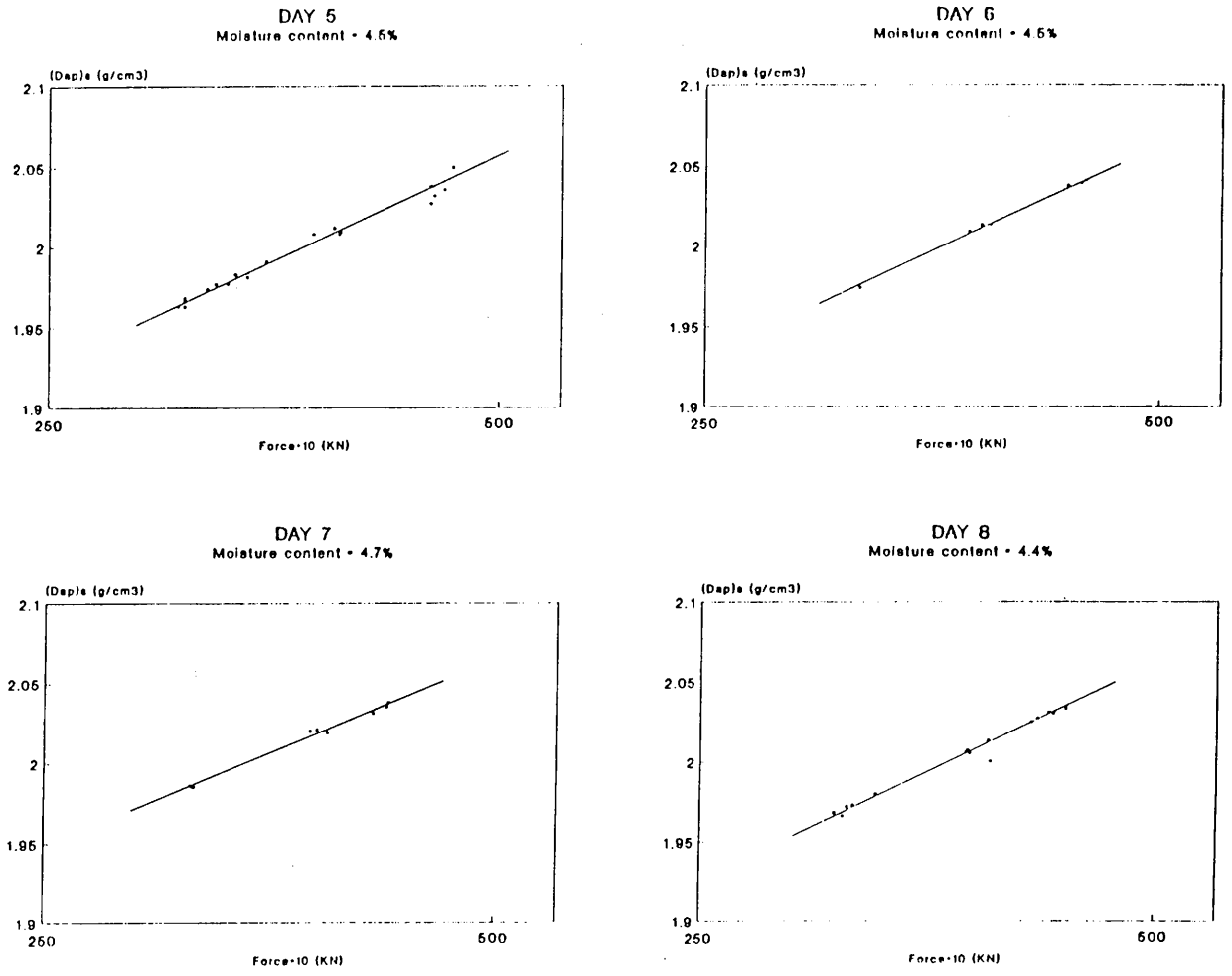


Figure 15.-Correlations between force, measured by the sensor, and dry bulk density determined by immersion in mercury.

The value to be observed in the correlation coefficients of these fits is so low because the range of variation in moisture content with which the experiments were carried out, is narrow (less than 0.004 kg of water/kg of dry solid), as a result of working on an industrial scale.

The bulk density prediction can be carried out from the signal recorded by the load sensor at the moment maximum pressure during the second pressing is reached, and moisture content of the spray-dried powder from the following equations:

$$M = 10^{(-1.29 * \log(H) + 0.48)} \quad (8)$$

$$b = 10^{(0.90 * \log(H) - 0.46)} \quad (9)$$

$$(Dap)_s = M * \log(7.63 * S + 0.44) + b \quad (10)$$

where:

$(Dap)_s$ : dry bulk density of the pressed piece in the sensor-monitored area ($g/cm^3$)
H : moisture content of the piece (kg of water/kg of dry solid)
S : signal received by the sensor at the moment maximum pressured is applied during the second pressing (digits)

By using the above-mentioned algorithm to predict bulk densities which have given rise to it according to the following scheme:

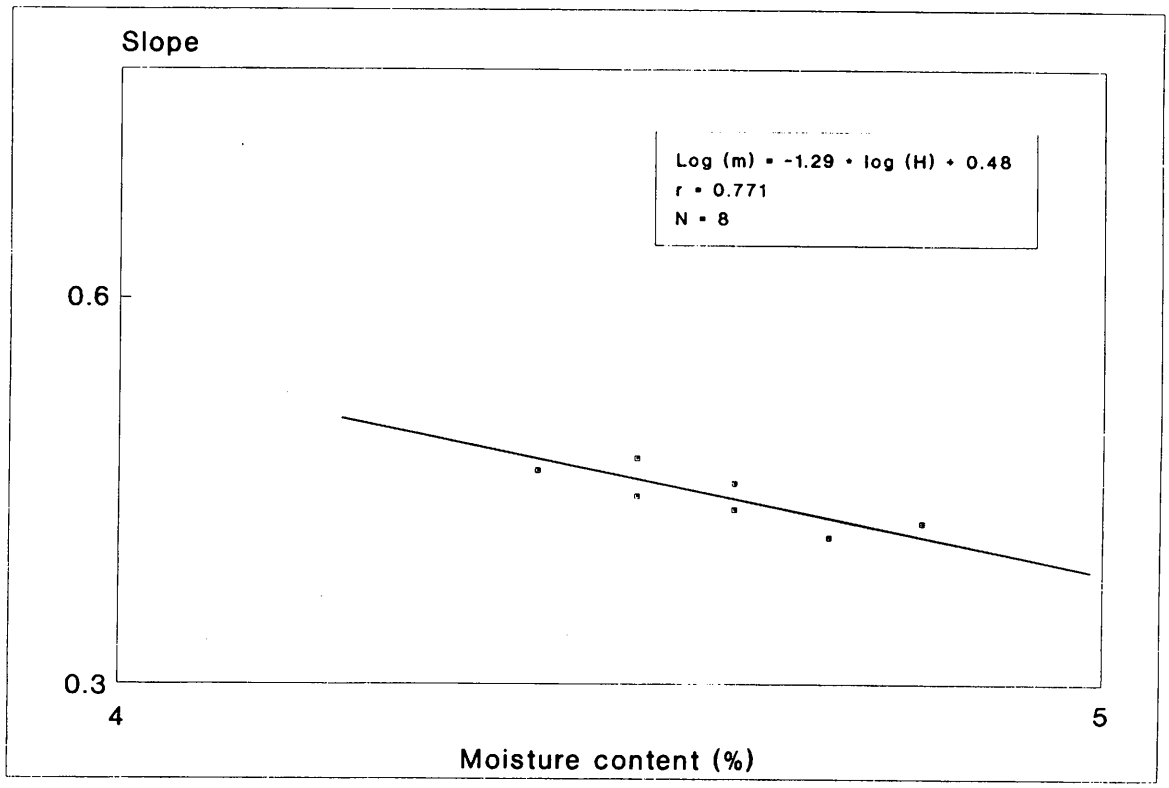


Figure 16.- Plot of the variation of the slope with moisture content, fitted to a straight line.

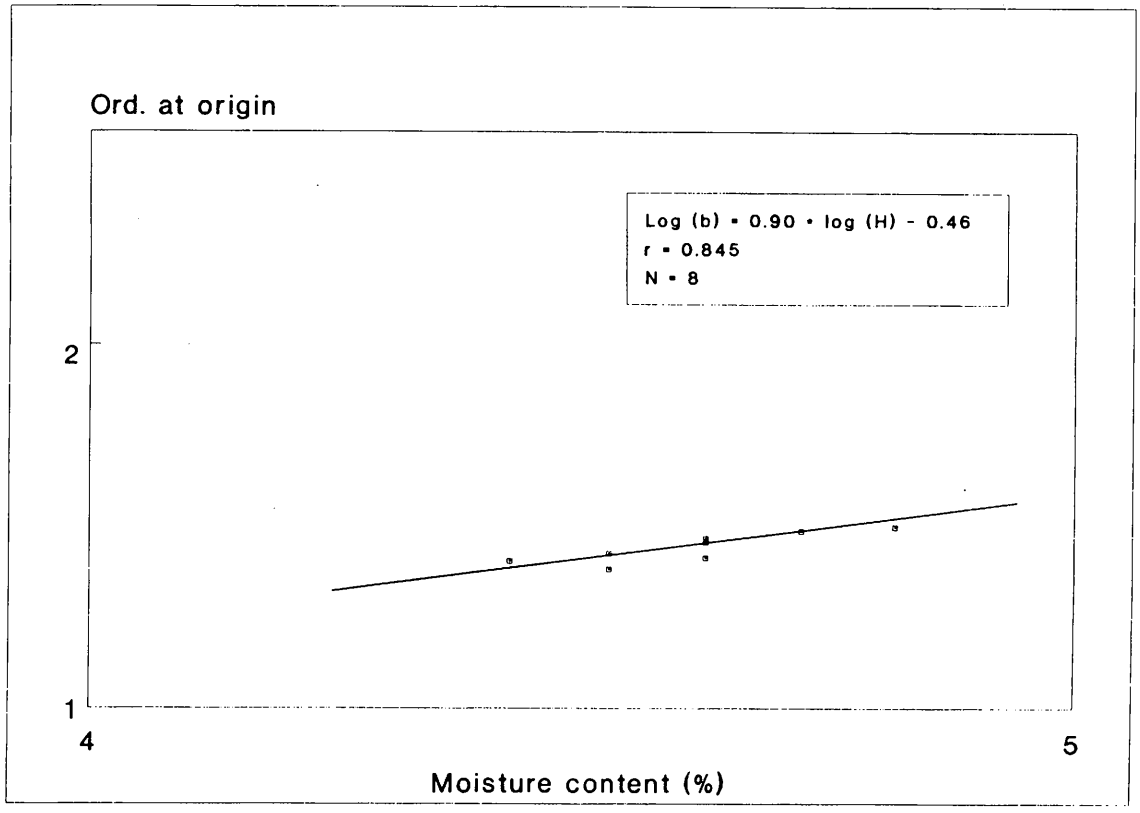


Figure 17.- Plot of the variation of the ordinate at the origin with moisture content, fitted to a strainght line.

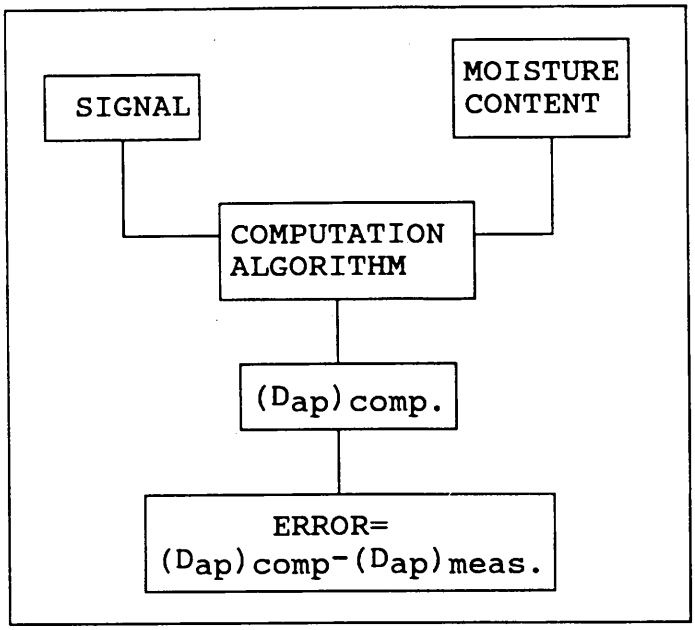


Figure 18.- Scheme of the process followed in evaluating the proposed method.

the following measurement distribution is found according to the computed errors:

| | % of measurements with an error less than : | | | |
|---|---|---|---|---|
| Δ Dap(gr/cm$^3$) | ±0.005 | ±0.01 | ±0.015 | ±0.02 |
| % of measurements | 55% | 93% | 99% | 100% |

Table III.- Total measurement distribution according to the computed errors.

## 10.- CONCLUSIONS.

The following conclusions may be drawn from the study conducted:

- The method for determining bulk density of the unfired ware by using load sensors, based on strain gauges, is accurate enough to be used in process control, since the observed error is 0.015 g/cm$^3$, which lies within the confidence interval required (0.03 g/cm$^3$)

- The extensometric method allows the spray-dried powder compression mode to be established, as well as determining bulk density, making it one of the fundamental instruments in studying this operation.

- Knowledge of compaction of the piece, in continuous operation and in true time, is necessary to reach a degree of automation in the pressing process which will enable dimensional characteristics to be kept more constant, and therefore also achieve greater, more constant finished product quality.

## 11.- REFERENCES.


(1) Estudios de pastas de gres para pavimentos.
A. Escardino, J.L. Amorós, J.E. Enrique.
Bol. Soc. Esp. Ceram. Vidrio, 20 (1), 17-24, (1981).

(2) Pastas de gres de monococción. Influencias de las variables de proceso en la calidad del producto acabado.
J.L. Amorós, A. Blasco, V. Beltrán, F. Negre, C. Arrébola.
Técnica Cerámica, 120, 1368-1384, (1984).

(3) La operación de prensado en la fabricación de pavimento por monococción. I Influencia de la naturaleza del polvo de prensas sobre las propiedades de la pieza en crudo.
J.L. Amorós, V. Bagán, Mª J. Orts, A. Escardino.
Bol. Soc. Esp. Ceram. Vidrio, 27 (5), 273-282, (1988).

(4) La operación de prensado de pavimentos por monococción. II Influencia de la naturaleza del polvo de prensas sobre las propiedades de la pieza en cocido.
J.L. Amorós, A. Moreno, Mª J. Orts, A. Escardino.
Bol. Soc. Esp. Ceram. Vidrio, 29 (3), 151-158, (1990).

(5) Tesis Doctoral, 1987.
Dpto. Ingeniería Química. Universidad de Valencia.
J.L. Amorós.

(6) Relación entre las variables de prensado y la velocidad de secado de la pieza moldeada
J.L. Amorós, A. Escardino, M.A. Gallego, F. Negre.
XXVII Reunión Anual de la Sociedad Española de Cerámica y Vidrio. Merida, Mayo (1987).

(7) Succión de líquidos por materiales cerámicos porosos.
V. Beltrán, A. Escardino, C. Feliu, M.D. Rodrigo.
Br. Ceram. Trans. J., Nº 87, 64-69, (1988).

(8) Cinética de la oxidación de la materia orgánica en productos cerámicos prensados.
A. Escardino, J.L. Amorós, V. Beltrán.
Actas del I Congreso Iberoamericano de Cerámica, Vidrio y Refractarios (S.E.C.V.), Vol. I, 317-326, (1983).

(9) Acuerdo Esmalte-Soporte I. Causas y factores de los que depende.
J.L. Amorós, F. Negre. A. Belda, E. Sánchez.
Técnica Cerámica, 178, 582-592, (1989).

(10) Rapid Sectional Density Measurement of Green PM Compacts.
K. Hummert, H. Dirkes, V. Arnhold.
Horizons of Powder Metallurgy, Part II, 735-745, (1986).

(11) Métodos de Difracción de Rayos X. Principios y Aplicaciones.
Joaquín Bermudez Polonio.
Ed. Pirámide, S.A. Madrid (1981).

(12) Quantitative X-Ray Spectrometry.
Ron Jenkins, R.W. Gould, Dale Gedcke.
Marcel Dekker, INC. (1981).

(13) Nondestructive Density Evaluation of PM Objects by Computer Tomography.
H. Heidt, J. Goibbels, A. Kettschan P. Reimers.
Horizons of Powder Metallurgy, Part II, Págs. 723-726. (1986).

(14) Ultrasonic Nondestructive Materials Characterization.
Robert E. Green, Jr.
Materials Analysis by Ultrasonics, 1-29.
Noyes Data Corporation (1987).

(15) Ultrasonic Characterization of Structural Ceramics.
Stanley J. Klina, George Y. Baaklim.
Materials Analysis by Ultrasonics, 112-121.
Noyes Data Corporation (1987).

(16) An Introduction to Measurements Using Strain Gages.
Karl Hoffman.
Hottinger Baldwin Messtechnick GmbH. Darmstadt (1987).

(17) Técnicas experimentales del control de la compactación de pavimentos y revestimientos cerámicos.
J.L. Amorós; V. Beltrán; A. Blasco; C. Feliu; M. Sancho-Tello.
Técnica cerámica nº 115, 1234-1246, (1983).

(18) A Safe and Fast Method for Testing Pressing Density.
Iberditan, S.A. Castellón (Spain).
TBI. Volumen 6, nº2, (1990).

(19) Compaction of Spray-Dried Powders.
Robert A. Youshaw and John W. Hallorah.
Ceramic Bulletin Vol. 61, nº2 (1982).

(20) Acuerdo esmalte-soporte III. Elasticidad de soportes y vidriados cerámicos.
J.L. Amorós; Mª J. Orts; A. Gozalbo; E. Montiel.
Técnica Cerámica, 180, 34-35, (1990).